8-12-2016

Sympathetic And Sensory Innervation And Activation Of Inguinal And Epididymal White Adipose Tissue

Jennifer Mendez

SYMPATHETIC AND SENSORY INNERVATION AND ACTIVATION OF INGUINAL AND EPIDIDYMAL WHITE ADIPOSE TISSUE

by

JENNIFER MENDEZ

Under the Direction of Aaron Roseberry, PhD

ABSTRACT

Studies have suggested the possibility that there is sensory (SS) afferent signaling from white adipose tissue (WAT) to the brain, which may play an important role in communication with the brain sympathetic nervous system (SNS) outflow to WAT. Therefore, we tested whether the SNS-SS feedback loop between the subcutaneous inguinal WAT (IWAT) and the epididymal WAT (EWAT) exists. These fat pads were chosen due to 1) their divergent role in manifestation of metabolic disorders with the IWAT being beneficial and the EWAT being detrimental, as well as 2) different lipolytic response to glucoprivic 2-deoxyglucose (2DG). By using retrograde tract tracers Fast Blue (FB) and Fluorogold (FG), we found that the IWAT is more innervated than EWAT by both the SS and SNS ganglia (T13-L3). Surprisingly, we found ~12-17% of double-labeled cells in the SNS and SS ganglia innervating fat depots, implying SNS-SS crosstalk loops between the IWAT and EWAT. Increased neuronal activation by 2DG was observed in the SNS ganglia to both IWAT and EWAT but not in the SS dorsal root ganglia. In addition, 2DG induced lipolysis in both fat pads with greater lipolytic properties in the IWAT as a result of higher density of the SNS-SS fibers. Collectively, our results show neuroanatomical reality of the IWAT and EWAT SNS-SS neural crosstalk with a coordinated control of lipolytic function.

INDEX WORDS: Lipolysis, 2-deoxyglucose, c-Fos, Fast Blue, Fluorogold, Dorsal root ganglia

SYMPATHETIC AND SENSORY INNERVATION AND ACTIVATION OF INGUINL AND EPIDIDYMAL WHITE ADIPOSE TISSUE

by

JENNIFER MENDEZ

A Thesis Submitted in Partial Fulfillment of the Requirements for the Degree of

Master of Science

in the College of Arts and Sciences

Georgia State University

2016

SYMPATHETIC AND SENSORY INNERVATION AND ACTIVATION OF INGUINAL AND EPIDIDYMAL WHITE ADIPOSE TISSUE

by

JENNIFER MENDEZ

Committee Chair: Aaron Roseberry

Committee: Bingzhong Xue

Laura Carruth

Vitaly Ryu

Electronic Version Approved:

Office of Graduate Studies

College of Arts and Sciences

Georgia State University

August 2016

ACKNOWLEDGEMENTS

I would like to thank Dr. Timothy Bartness for giving me the opportunity to be a part of his lab. I am very thankful and grateful to have been mentored by him and for his support. I will continue to carry his advice and the invaluable knowledge and that he instilled in me throughout the years to come.

I would also like to thank Dr. Aaron Roseberry for taking me in as my advisor on short notice. As well as Dr. Bringxhong Xue and Dr. Carruth for being a part of my committee and for their advice on this project. My greatest gratitude to Dr. Vitaly Ryu for all of his patience, help, and advice on the completion of my thesis. I would also like to thank my lab peers for the years of friendship and collaborations made along the way.

Finally, I would like to thank my loving and caring mother, Lorena, for her encouragement. I would also like to thank my uncle, Mauricio, and my two beautiful cousins, Kaedee and Shelby, and my friends for all their support throughout the years. I hope that I have opened their eyes and sparked a love and curiosity for science in each one them as Tim did in me.

TABLE OF CONTENTS

LIST OF FIGURES

1 INTRODUCTION

1.1 Background

Today, approximately 30% of the world's population are either obese or overweight and the number has doubled since 1980 (24). In 2012, in the U.S. alone, more than one third of the population were considered obese (26). Obesity is the cause a variety of secondary health consequences such as cardiovascular disease, type II diabetes, stroke, hypertension (17, 27, 28, 40). Along with these health consequences come an economic burden. In 2008, the U.S medical costs associated with this disease was estimated to be $147 billion dollars(15). Obesity can result from a variety of factors including genetics and behavior. Most commonly it is due to excess energy being consumed compared to that which is being expended. In mammals, the majority of surplus energy is being stored in the form of triacylglycerols (TAGs) in various WAT depots which are located subcutaneously, around the upper and lower body regions and abdomen, as well as internally around vital organs.

1.2 Lipolysis induced by the SNS

During times of increased energy demands lipid mobilization occurs. The sufficiency of the activation of the sympathetic nervous system (SNS) innervation of WAT for lipid mobilization was demonstrated in *ex vivo* studies with electrical stimulation of the intact SNS nerves innervating EWAT which resulted in increased concentration of free fatty acids in the incubation medium (13). In addition, it was demonstrated that the removal of the sole source of circulating epinephrine by bilateral demedullation fails to block lipolysis (2, 14) whereas the SNS innervation of WAT is sufficient and necessary for the beginning of lipolysis. The SNS postganglionic nerves release norepinephrine (NE) which binds to beta adrenergic receptors (β-AR), which further activates a cascade of intercellular signaling events initiating lipolysis, thus

the SNS is the principal initiator for lipolysis and the balance between the stimulation of lipolysis by β-ARs and its inhibition by α2-AR imposes the degree of lipolysis(12, 18). When NE binds to β3-ARs it activates the G coupled GTP binding protein GS. This activation increases cAMP by activating adenylyl cyclase and results in stimulation of protein kinase A (PKA) which phosphorylates two key players in lipolysis, hormone sensitive lipase (HSL) and perilipin A (1, 11, 19), an adipocyte bound protein that prevents hydrolysis of the stored fat. When perilipin A is phosphorylated, it acts as a scaffolding protein exposing the lipid droplet for the translocation of HSL (30) from the cytoplasm to the cell wall, to facilitate in lipolysis to undergo hydrolysis of triacylglycerol to result in free fatty acids (FFAs) and glycerol. There are two rate-limiting enzymes considered for lipolysis, which have different intracellular cascades for the hydrolysis of TAG. For stimulated lipolysis (i.e., SNS/NE-stimulated) pHSL is the rate-limiting enzyme whereas under basal lipolysis (i.e., non-SNS/NE-stimulated) ATGL is the rate-limiting enzyme. During stimulated lipolysis ATGL assists in hydrolysis of TAG by removing, a FA to produce diacylgylercol (DAG), which frees another FA by pHSL to produce monoacylglycerol (MAG), where the last FA is removed by MAG lipase.

1.3 SNS Innervation of WAT

The mobilization of WAT is not homogenous, lipolysis occurs at different lipolytic rates, depending primarily on where the adipose tissue is located. We observed this while studying the reversal of a naturally-occurring seasonal obesity in Siberian hamsters where obesity (body fat of ~50%) induced by long summer days is reversed when exposed to short “winter-like” days (body fat of ~20%) (5, 8, 22, 37). Internal WAT pads [*e.g.*, retroperitoneal WAT (RWAT), and

epididymal WAT (EWAT)] are mobilized at a higher degree compared to the externally located subcutaneous WAT [e.g., dorsosubcutaneous WAT (DWAT), and inguinal WAT (IWAT) (3, 6, 7). The SNS innervation of WAT was demonstrated histologically, with innervation of the SNS marker tyrosin hydroxylase (TH) immunoreactivity (-ir) (33). Direct evidence of the SNS innervation was observed in the postganglionic SNS ganglia by the monosynatpic retrograde tract tracer, Fluorogold (FG), both intra-IWAT and intra-EWAT(38). Functionally, selective surgical and chemical SNS denervation of WAT completely blocks lipolysis emphasizing the master role of the SNS innervation in triggering lipolytic responses (4, 39). Using a retrograde viral tract tracer, pseudorabies (PRV), we previously identified the central origins of the SNS outflow to WAT by, in Siberian hamsters (2, 34, 35) and Sprague-Dawley rats (2). This has further been investigated in various fat pads including IWAT, EWAT, RWAT, and MWAT (4, 9, 25, 29, 31). Collectively, our viral studies revealed a number of the central sites implicated in the SNS efferent outflow to above-mentioned fat pads as well as sensory system (SS) afferent inflow from those fat pads to the brain (2, 29). Importantly, many areas contained both PRV152 and H129 (SNS + SS colocalization) viruses suggesting long SNS-SS feedback circuits (2, 9, 29). Notably, some areas exhibited greater levels of infection indicating SNS drive from the brain to WAT is fat pad-specific. In concordance with this, we later confirmed differential SNS drives to WAT by measuring NE turnover (NETO) levels in Siberian hamsters in response to various metabolic stimuli (10) (*i.e.,* cold exposure, food deprivation, glucoprivation, and central stimulation with melanocortins).

1.4 SS Innervation of WAT

Histologically, two proven sensory neuropeptides, substance P and calcitonin gene-related peptide (CGRP), was found in the WAT of Sprague Dawley rats while CGRP was found in the IWAT and EWAT of the Siberian hamster, inferring WAT innervation by the SS (32, 33). However, direct evidence of the SS innervation of WAT was first observed after injecting the retrograde tract tracer, True Blue, into the IWAT and DWAT of laboratory rats which resulted in labeling of pseudounipolar neurons in DRG associated with the concrete fat depot (16). Recently, more focus has been on understanding the SS role in WAT brain communication. Using the same conventional tract tracer and viral methodology, we revealed the central SS circuits from WAT of not only Siberian hamsters, but of Sprague-Dawley rats as well (16, 23, 29). There is strong evidence suggesting that neural feedback loops may exist between WAT SS afferents from and the SNS efferents to WAT. This was demonstrated by identifying the SS innervation from WAT to the brain that shared many identical sites across the neuroaxis with the neurons sending the SNS outflow to WAT (25, 29, 36). Studies involving excitatory effect of adipokine leptin on the SS afferents emanating from WAT, support the suggestion that leptin plays a novel role as a SS paracrine factor in WAT by informing the brain of lipid stores in WAT and does so in a fat pad-specific manner (23). It is also suggested that lipolysis within WAT may activate the SS afferent signaling. In support of the latter, intraperitoneal (i.p.) injections of 2-deoxyglucose (2DG) a non-metabolizable glucose analog, and intra-WAT injections CL, a beta-adrenergic agonist, rapidly increase neurophysiological spike activity in WAT SS fibers (36). In this regard, surgical removal or the SS denervation of one fat depot followed by compensatory increase in fat mass across the remaining fat depots emphasizes the importance of the SS signaling (20, 32).

1.5 Purpose of experiment

Because it is known that IWAT and EWAT respond to lipolytic stimuli differently and are located differently in the hamsters, these two are a good model to study activation of the SS and SNS innervation of WAT. In our previous studies, the use of Fast Blue (FB) and Fluorogold (FG) tract tracing enabled us to identify mostly separate SNS innervation within the IWAT and EWAT. Here, we hypothesize that IWAT as well as EWAT both will share SS and SNS innervation. When given the lipolytic stimuli, 2DG, IWAT has a higher SNS drive compared to that of EWAT (10), implying that the first should have a higher SNS neuronal activation and as a result, a higher lipolytic rate. Additionally, given that the SS afferent signaling from WAT to the brain may inform the brain of lipid stores within WAT (23), we hypothesize that the greater SNS drive to IWAT might result in greater SS feedback.

2 MATERIALS AND METHODS

All procedures were approved by the Georgia State University Institutional Animal Care and Use Committee and are in concordance with Public Health Service and United States Department of Agriculture guidelines.

2.1 Animal Model

Adult male Siberian hamsters, *(Phodopus sungorus,* ~3-4 mo old) were single-housed after being selected from our breeding colony. Animals were kept in a long day photoperiod (16:8-h light-dark cycle) at 21 ± 2 °C, with relative humidity at 50 ± 10%) with *ad libitum* access to water and rodent chow. Hamsters were single-housed for 7–10 days before all procedures.

2.2 SNS and SS innervation of WAT

Siberian hamsters (n = 36) were anesthetized with 2% isoflurane. The skin around the haunch area over the IWAT pad was shaved and wiped with 70% ethanol and then 10% povidone iodine solution (Ricca Chemical, Arlington, TX) repeatedly, finishing with povidone iodine. An incision was made around this haunch to expose the IWAT. Similarly, we made an incision in the peritoneal wall close to the EWAT to expose the fat pad for injections. Once exposed, fat pads were maintained moist for the entire procedure. The two tract tracers, 2% FG (Fluorochrome, Denver, CO) and 1% FB (EMS-CHEMIE GmbH, Gross-Umstadt) were injected unilaterally into eight separate sites across the IWAT pad (1 μl per locus for a total of 8 μl) and into six separate sites across the EWAT pad (1 μl per locus totaling 6 μl). After each injection, the needle was held in place for 1 min to minimize reflux up the outside of the needle. The peritoneal wall was closed with sterile sutures and the skin incision was closed with sterile

wound clips. In order to minimize the risk of bacterial infection nitrofurozone (nz Puffer; Hess & Clark) was applied locally on the incision. To ensure proper labeling, tracers were switched between each group to account for differential labeling between tracers. Two weeks post injections of tracers hamsters were perfused for histological analyses as described below.

2.3 SNS and SS activation of WAT

Hamsters (n=36) were divided into three groups based on an average body weight of ~40 g. On the day of the procedure, animals were transferred to the experimental room and were allowed to acclimate for at least 2 h to reduce any stress associated with the transfer. After acclimation, animals were depouched and food deprived. Two hours later the animals were given the appropriate treatment of i.p. injections of saline or 2-DG (500 mg/kg or 1000 mg/kg). The 2 hour period post depouching was performed to minimize any disruption in sympathetic activity due to the depouching.

2.4 Histological preparation and harvesting of ganglia

Hamsters were overdosed with pentobarbital sodium (300 mg/kg ip) and perfused transcardially with heparinized (0.9%) saline and paraformaldehyde (4%) in 0.1 M phosphate buffer (pH 7.4). DRG and the SNS ganglia associated with spinal vertebrae T12-L3 were carefully removed and debrided from the epineurium, post fixed in the same fixative for 20 min, and then transferred to a sucrose solution (18%) with 0.1% sodium azide where it was stored at 4 °C for 2 d. The ganglia were sectioned longitudinally at 20 μm on a freezing stage cryostat and collected onto gel-coated slides (Superfrost Plus, VWR International, West Chester, PA) in a series of three (with every forth section on the same slide), immediately after being sliced and stored at 4 °C until processing for immunohistochemistry (IHC).

2.5 c-Fos and Fluorogold IHC

The ganglia sections were rinsed in PBS (3 ×10 min), followed by a 1 h incubation in 5% normal horse serum (NHS) (1:200; Vector Laboratories, Burlingame, CA) in PBTx (PBS containing 0.3% Triton X-100). Sections were then incubated in primary rabbit anti-c-Fos (1:500 for DRG and 1:2000 for SNS ganglia; sc-52; Santa Cruz Biotech, Santa Cruz, CA) antibody with 10% NHS in PBTx with 0.3% sodium azide for 2 d at 4 °C. Next, the sections were rinsed with PBS (3×15 min), then incubated for 3 h in Alexa 594 conjugated streptavidin anti rabbit (1:400; Molecular Probes, Eugene, OR) with 10% NHS in PBTx with at 4 °C. For IHC controls, the primary antibody was either omitted or reabsorbed with the immunizing peptide overnight at 4 °C thus resulting in negative immunostaining (data not shown). Following subsequent rinses with PBS (4×15 min), the sections were incubated in another primary rabbit anti Fluorogold (1:20,000; Fluorochrome, Denver, CO) antibody followed by the secondary Alexa 488 conjugated streptavidin anti rabbit (1:400; Molecular Probes, Eugene, OR) antibody. Sections were cover slipped using ProLong Gold Antifade Reagent (Molecular Probes) for future analysis and quantification.

2.6 Western blot analysis

For the western blot experiment, IWAT and EWAT were immediately excised from animals after injection with pentobarbital sodium (300 mg/kg) prior to perfusion. Tissues were then snap frozen with liquid nitrogen and stored at -80 °C until processed. The fat pads were then minced and placed in a microcentrifuge tube containing zirconium oxide beads and a 2:1 ratio of Homogenization buffer [50 mM HEPES, 100 mM NaCl, 10 % SDS, 2 mM EDTA, 0.5 mM DTT, 1 mM benzamidine] and both protease inhibitor cocktail (Calbiochem, EMD Chemicals,

Gibbstown, NJ), and phosphatase inhibitor cocktail (Thermo Fischer Scientific, Rockford, IL). Tubes were inserted into the bullet blender for 2 x 1 min to break down the tissue and then centrifuged for 10 min at 13,000xg. The supernatant was then collected and extra aliquots were stored in -80 °C for future use. Protein concentration for each sample was determined by bicinchoninic acid protein assay kit (Thermo Fisher Scientific, Rockford, IL) and used to determine the amount of 4X Loading buffer and Millipore water to add to 10 μg of protein sample for SDS processing. The samples were then heated at 95 °C for 5 min, loaded on to a low-bis SDS-PAGE [10.0 %:0.08 % acrylamide:bis] and then underwent electrophoresis. The gel was then transferred to PVDF membranes for immunoblotting. Once immunoblotting was completed each membrane was cut in the designated area so that we could stain for the specific protein (pHSL, HSL, and the beta actin). Membranes were washed 2x10 min in Tris-buffered saline (TBS), blocked for 2 h in a in a blocking solution (4% nonfat dry milk in TBS), then incubated for 48 h in a primary antibody of either HSL, pHSL and β-actin (each 1:1000; Cell Signaling Technology, Danvers, MA) at 4 °C. After primary antibody incubation membranes were washed 3x5 min with TTBS, then incubated in secondary goat anti-rabbit IgG HRP-linked antibody, 1:1000; Cell Signaling Technology, Danvers, MA) for 2 h at 4 °C. The membranes were rinsed 3x10 min in TBST and then incubated with LumiGLO chemiluminescent kit (Cell Signaling Technology, Danvers, MA) to visualize bands on a gel imager.

2.7 Quantitative and statistical analysis

The intensity of Western blot bands was quantified based on optical densitometry measurements using ImageJ (US National Institutes of Health, Bethesda, MA). Ratio values of proteins and the controls, pHSL/actin and HSL/actin, were collected and then used for the ratio of total pHSL/HSL.

Images were view and captured under 100X and 200X magnification with the Olympus BX41 microscope and the appropriate filters for FB, Alexa 594, and Alexa 488. FB, FG, and c-Fos-ir neurons were considered positive based on cell size, shape, and fluorescent intensity. The acquired images were adjusted by contrast, brightness, sharpness, and overlaying of double-labeled neurons by Adobe 250 Photoshop CS5 (Adobe Systems, San Jose, CA, USA).

All statistical analysis were carried out using NCSS (version 2007, Kaysville, UT). Data were analyzed by one-way repeated measures analysis of variance (ANOVA) followed by the post-hoc Bonferroni's and Holm-Sidak's tests using. Statistical significance was set at $P<0.05$ and all values are presented as mean ±standard error of the mean.

3 RESULTS

3.1 SS Innervation and Activation of WAT

The dual microinjections of the conventional tract tracers FG and FB intra-IWAT and intra-EWAT appeared at the T12-L3 DRG (Fig. 2). Total numbers of single-labeled as well as double-labeled cells in the DRG innervating fat pads, were given as an absolute numbers and their total percentages (Fig 2A, B). The DRG exhibited a differential pattern of innervation from both fat pads with the most innervation coming from the lumbar L1-L3 (Fig 2B). The number of DRG single labeled neurons innervating IWAT was significantly greater as compared with that innervating EWAT at T13-L3 ($P<0.05$; Fig. 2B) with ~2-fold ($P<0.05$; Fig. 2C). In addition, the percentages of single labeled neurons were significantly greater in DRG associated with the IWAT as compared with EWAT at T12-L3 ($P<0.05$; Fig. 2A). Notably, the percentile number of double-labeled cells innervating both fad pads, was ~12-17% for each SS ganglia (Fig 2B).

The number of c-Fos-ir cells in FG (from EWAT) and FB (from IWAT) labeled neurons were distributed across T12-L3 DRG (Fig. 3). Both doses of 2DG used in the study failed to induce neuronal activation in the DRG innervating the IWAT except for the L3 ganglion where 2DG at 500 mg/kg tended to significantly increase the percentile number of neurons compared with the saline group ($p=0.059$; Fig. 3A). Notably, the percentile number of activated neurons, as indicated by c-Fos immunostaining related to the highest 2DG dose (1000 mg/kg), was markedly lower as compared to the lower dosage ($p<0.05$; Fig. 3A). Similarly, there were no significant alterations in the numbers of c-Fos-ir cells innervating the EWAT for the only exception of L1 DRG where both doses of 2DG significantly decreased c-Fos-ir in comparison with that in the saline group ($p<0.05$; Fig. 3B).

3.2 SNS Innervation and Activation of WAT

The dual microinjections of the conventional tract tracers FG and FB intra-IWAT and intra-EWAT appeared at the T12-L3 SNS ganglia (Fig. 5). Total numbers of single-labeled as well as double-labeled cells in the SNS ganglia innervating fat pads, were given as an absolute numbers and their total percentages (Fig 5A, B). The SNS exhibited a differential pattern of innervation from both fat pads with the most innervation coming from the lumbar T13-L2 (Fig 5B). The number single labeled neurons in the SNS ganglia innervating IWAT were significantly greater as compared with that innervating EWAT at L1-L2 ($P<0.05$; Fig. 5B) with ~2-fold ($P<0.05$; Fig. 5C).). In addition, the percentages of single labeled neurons were significantly greater in DRG associated with the IWAT as compared with EWAT at T12-L3 ($P<0.05$; Fig. 5A). In addition, the percentile number of double-labeled cells innervating both fad pads was ~12-16% for each SNS ganglia (Fig 5B).

The number of c-Fos-ir cells in FG (from EWAT) and FB (from IWAT) labeled neurons were distributed across T12-L3 DRG (Fig. 6). 2DG induced a dose response increase of activation in the SNS to IWAT in ganglia T13 ($p < 0.05$, Fig 6A). Additionally, in IWAT, both dosages of 2DG (500 mg/kg and 1000 mg/kg) had a significant increase in SNS activation compared to the control group in SNS ganglia L1 ($p < 0.05$, Fig 6A). EWAT exhibited a significant increase in SNS activation in both T13 and L1 in the high dose of 2DG compared to the saline group as well as in T13 compared with the low dose of 2DG ($p < 0.05$, Fig 6B). 2DG at1000 mg/kg, but not at 500 mg/kg, significantly increased c-Fos-ir in double labeled cells at T13 SNS ganglion in comparison with the control group ($p < 0.05$, Fig 6C).

3.3 Effect of 2DG on Lypolytic Activity in the WAT

To ensure that 2DG was metabolizing in the animals accordingly we measured the blood glucose levels (Fig 7). Both doses of 2DG (500 mg/kg and 1000 mg/kg) significantly increased blood glucose levels in a dose-dependent manner with the highest increase by the latter dose ($p<0.05$; Fig. 7). Both IWAT and EWAT exhibited a dose-dependent significant increase in lipolysis indicated by the pHSL/HSL ratios compared with the saline group and this increase was significantly greater in the IWAT in comparison to EWAT for each treatment doses of 2DG ($p<0.05$; Fig. 8D). There were no significant change in lipolysis following the saline treatment ($p<0.05$; Fig. 8D). The percent values of pHSL/HSL had the same pattern; that is, 2DG dose-dependently and markedly increased lipolysis in the WAT with the higher increase in the IWAT ($p<0.05$; Fig 8C). In addition, Saline administration did not have any effect on lipolysis in both fat depots (Fig. 8C).

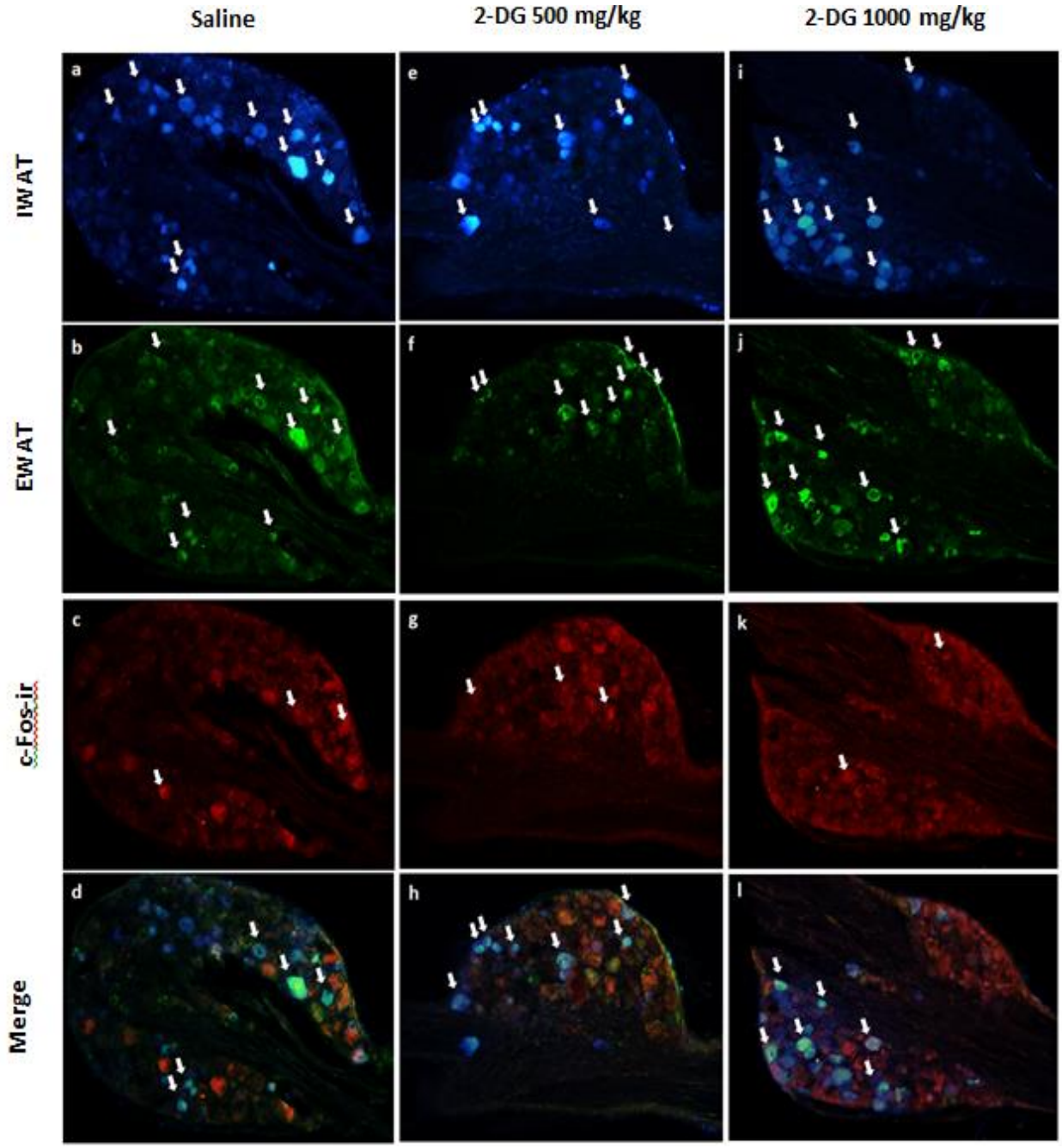

Figure 1: *Representative picture of Innervation and Activation of DRG to WAT. Photomicrograph illustrating labeling Sensory ganglia (DRG) L1 at 200X. Labeling of DRG after tract tracer injections in IWAT (blue) and EWAT (green). 2DG induced activation of DRG neurons a-d: Saline group, e-h: 2-DG 500mg/kg, i-l: 2-DG 1000 mg/kg. Scale bars = 50 μm.*

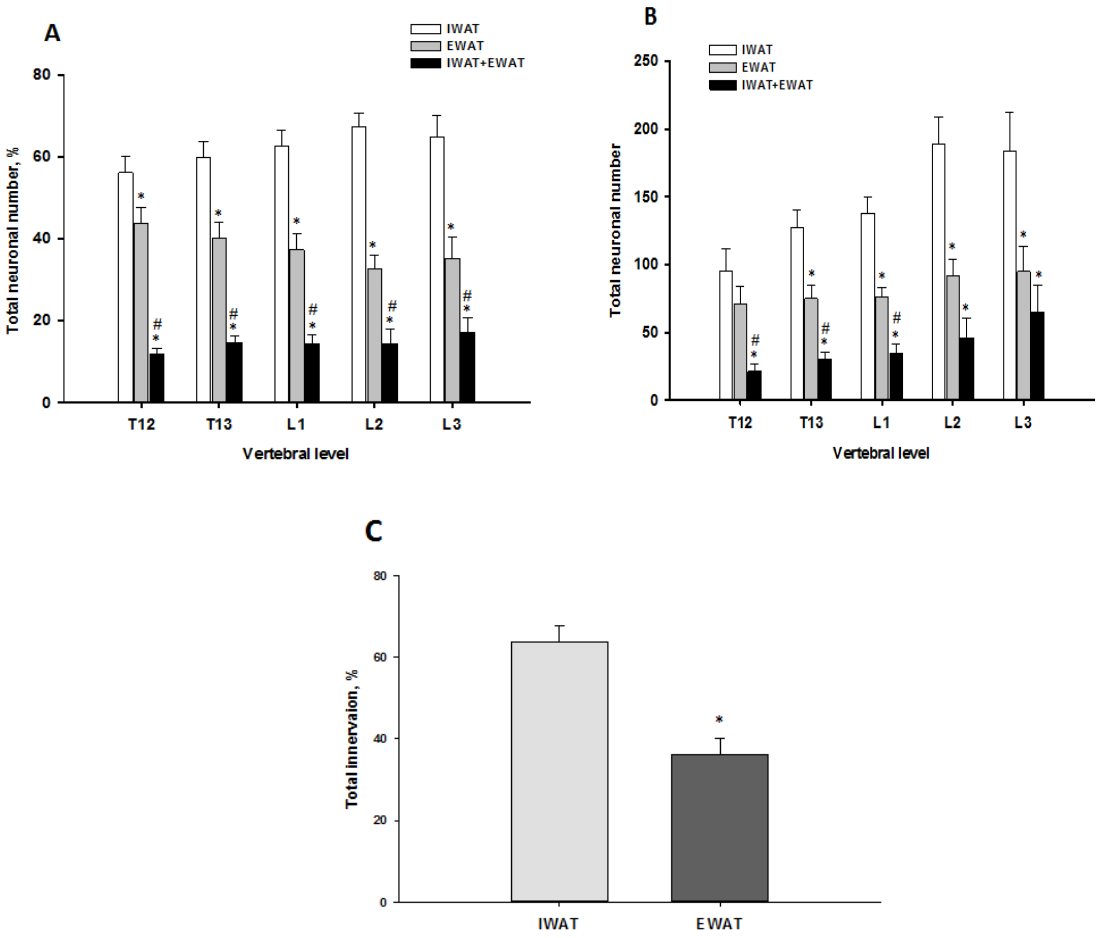

Figure 2: *Distribution of SS Innervation of DRG to WAT.*
*Distribution of IWAT and EWAT labeled cells in the DRG at the vertebral level T13-L3. A: Total percent of IWAT and EWAT. B: Total neuronal number of IWAT and EWAT. C: Quantification of percent total labeled SS innervated neurons to IWAT and EWAT. *P<0.05 vs IWAT, #P<0.05 vs EWAT.*

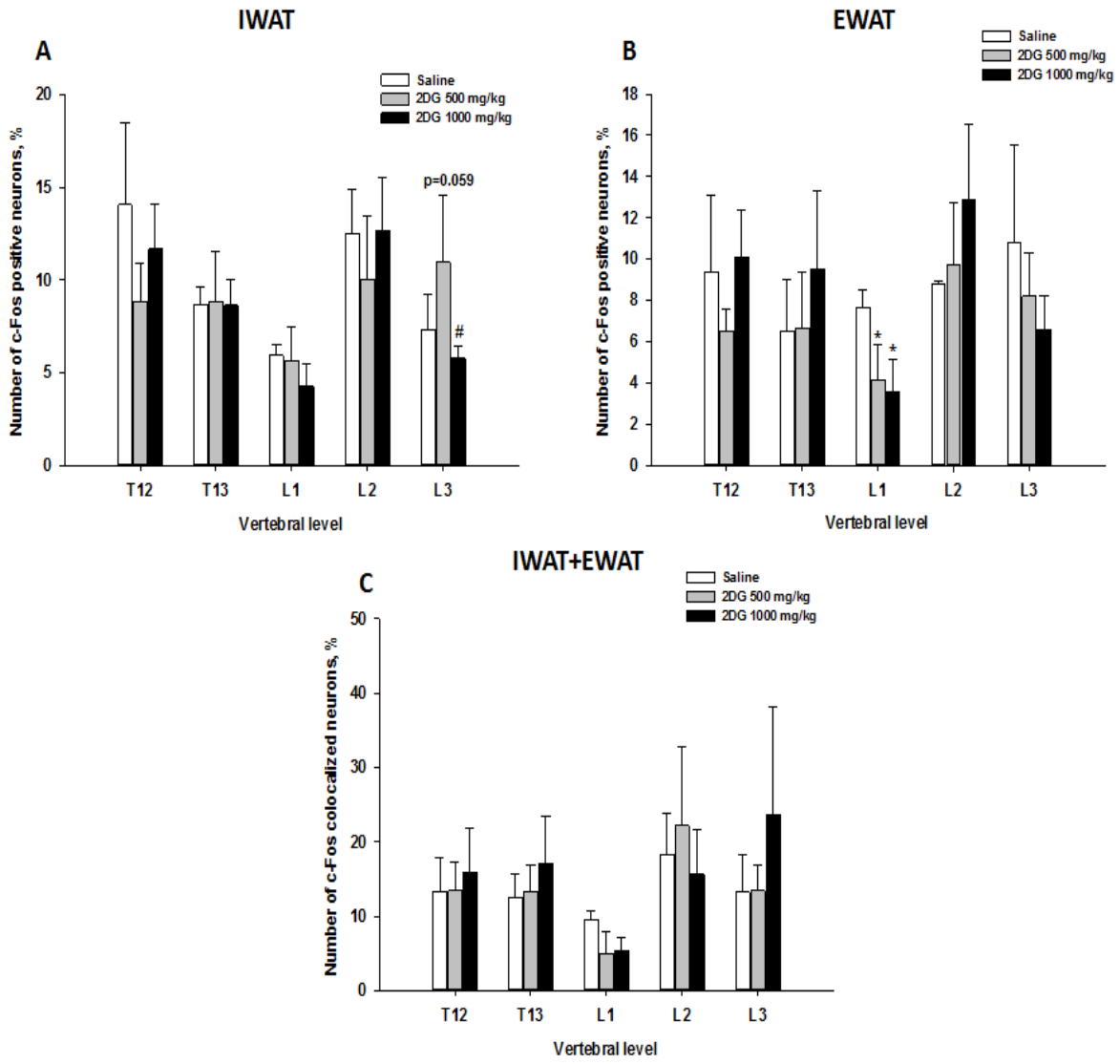

Figure 3: *Distribution of SS Activation of DRG to WAT.*
*2DG induced activation of DRG neurons innervating WAT at the vertebral level T13-L3. A: Percent of c-Fos-ir positive neurons innervating IWAT. B: Percent of c-Fos-ir positive neurons innervating EWAT C: Percent of c-Fos-ir positive neurons innervating IWAT+IWAT DB labeled cells*P<0.05 vs Saline, #P<0.05 vs 500mg/kg 2DG.*

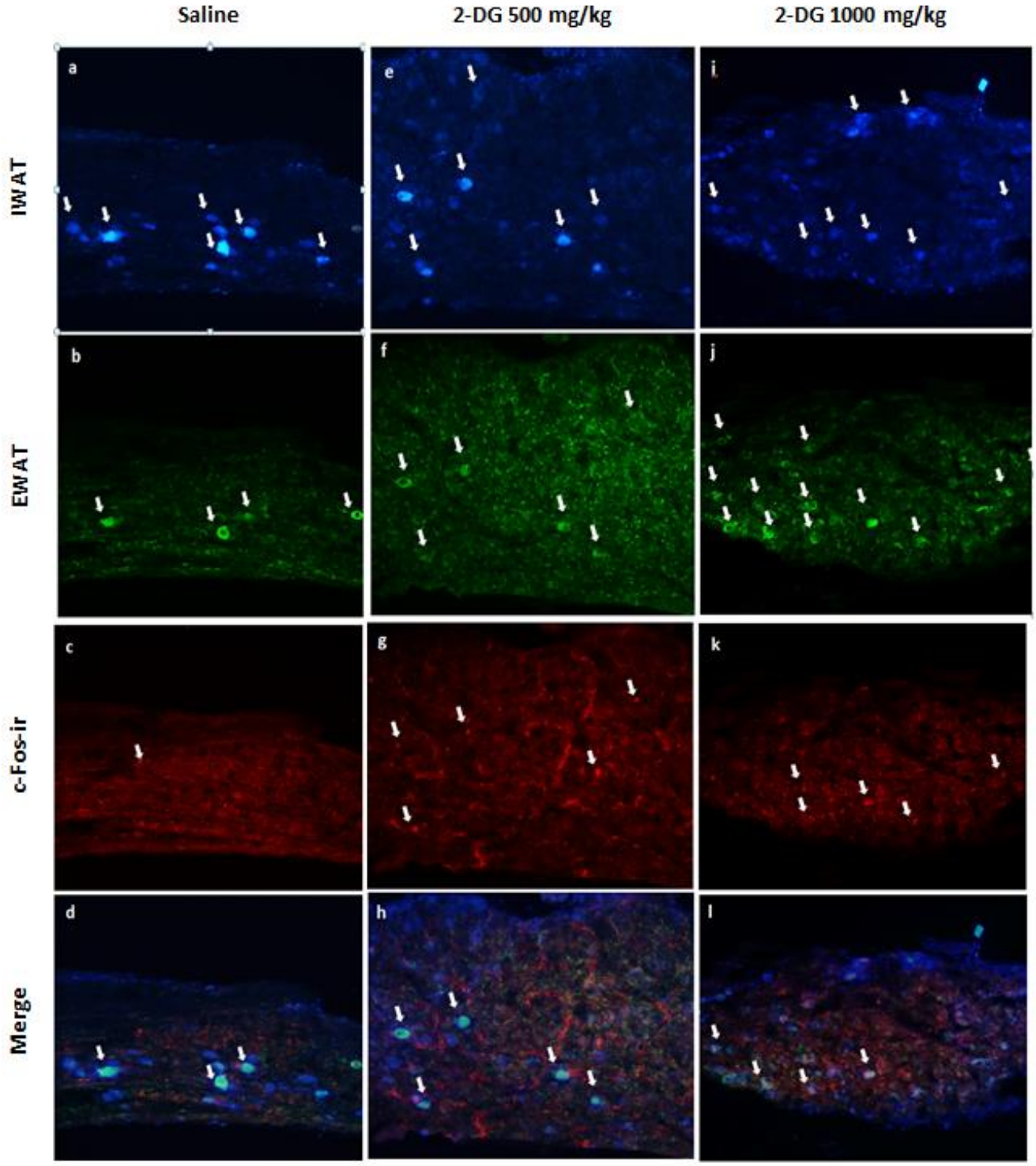

Figure 4: *Representative picture of Innervation and Activation of Sympathetic Ganglia to WAT.*

Photomicrograph illustrating labeling sympathetic ganglia (DRG) T13 at 200X. Labeling of sympathetic ganglia after tract tracer injections in IWAT (blue) and EWAT (green). 2DG

induced activation of sympathetic ganglia. a-d: Saline group, e-h: 2-DG 500mg/kg, i-l: 2-DG 1000 mg/kg. Scale bars = 50 µm.

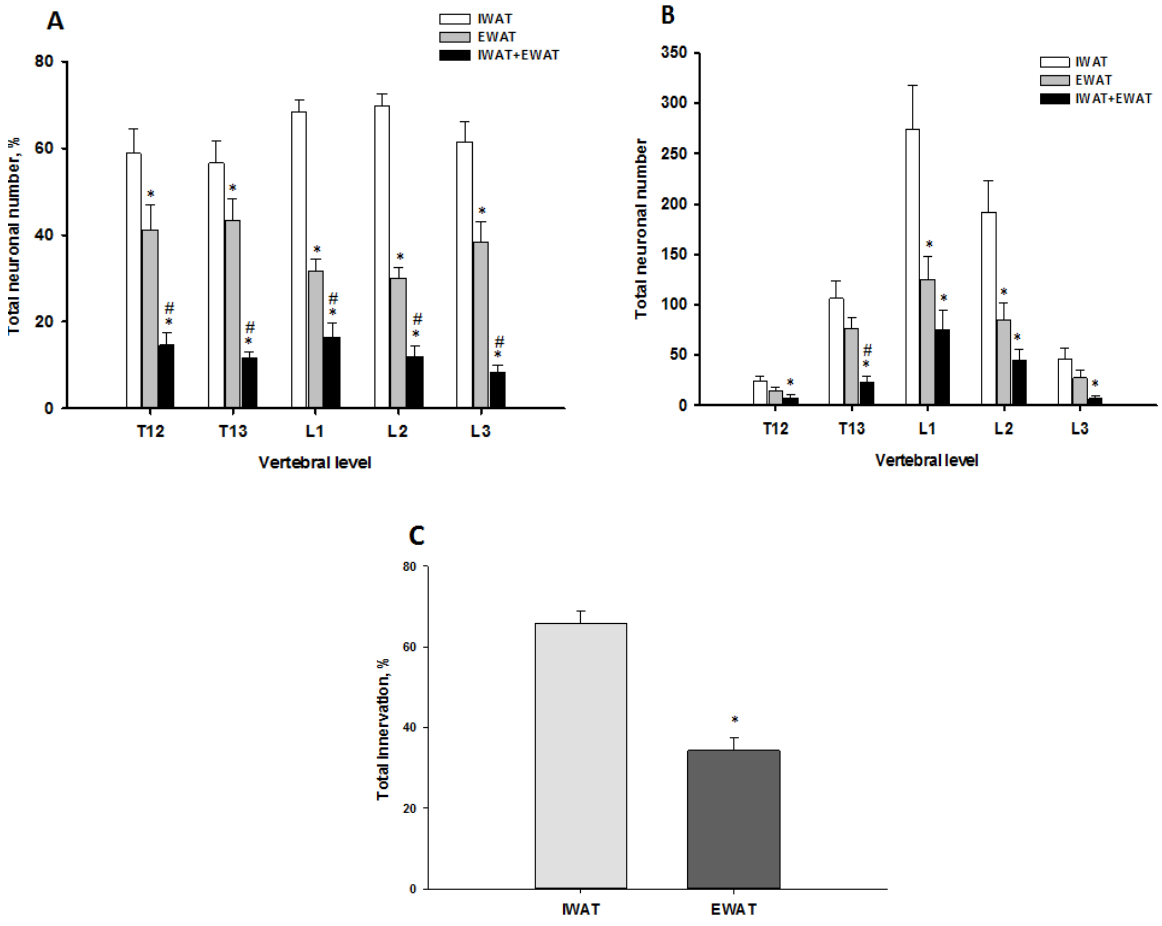

Figure 5: *Distribution of SNS Innervation of Sympathetic Ganglia to WAT. Distribution of IWAT and EWAT labeled cells in the SNS ganglia at the vertebral level T13-L3. A: Total percent of IWAT and EWAT. B: Total neuronal number of IWAT and EWAT. C: Quantification of percent total SNS labeled neurons to IWAT and EWAT. *P<0.05 vs IWAT, #P<0.05 vs EWAT.*

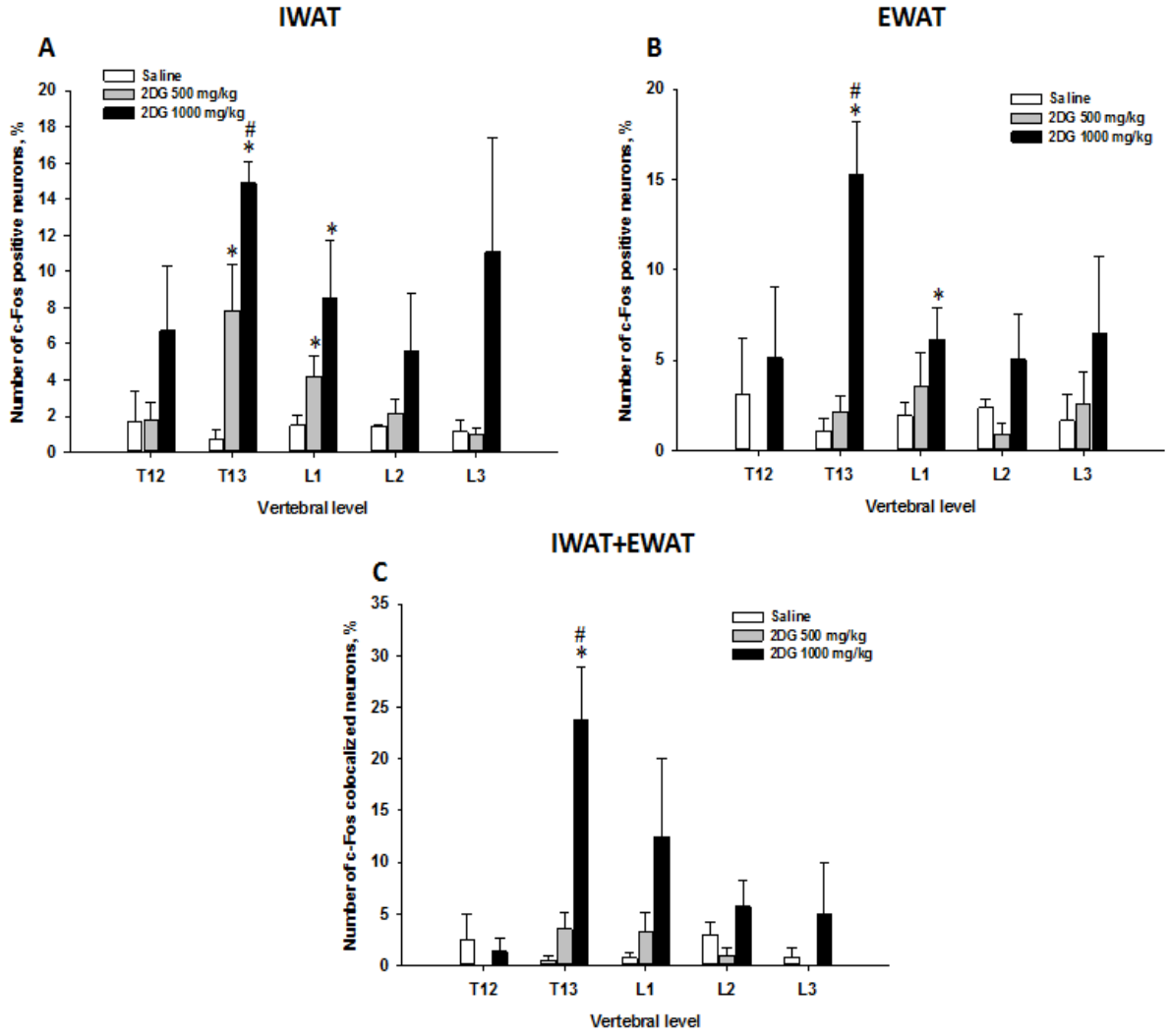

Figure 6: *Distribution of SNS Activation of Sympathetic Ganglia to WAT.*
*2DG induced activation of SNS neurons innervating WAT at the vertebral level T13-L3. A: Percent of c-Fos-ir positive neurons innervating IWAT. B: Percent of c-Fos-ir positive neurons innervating EWAT C: Percent of c-Fos-ir positive neurons innervating IWAT+IWAT DB labeled cells*P<0.05 vs Saline, #P<0.05 vs 500mg/kg 2DG.*

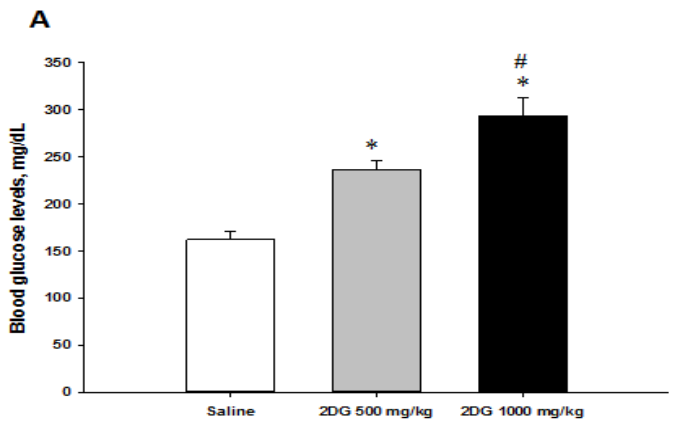

Figure 7: *Plasma Glucose.*
*Plasma glucose from hamsters given i.p injections of 500 mg/ kg and 1000 mg/kg 2DG and saline vehicle. *P<0.05 vs Saline, #P<0.05 vs 500mg/kg.*

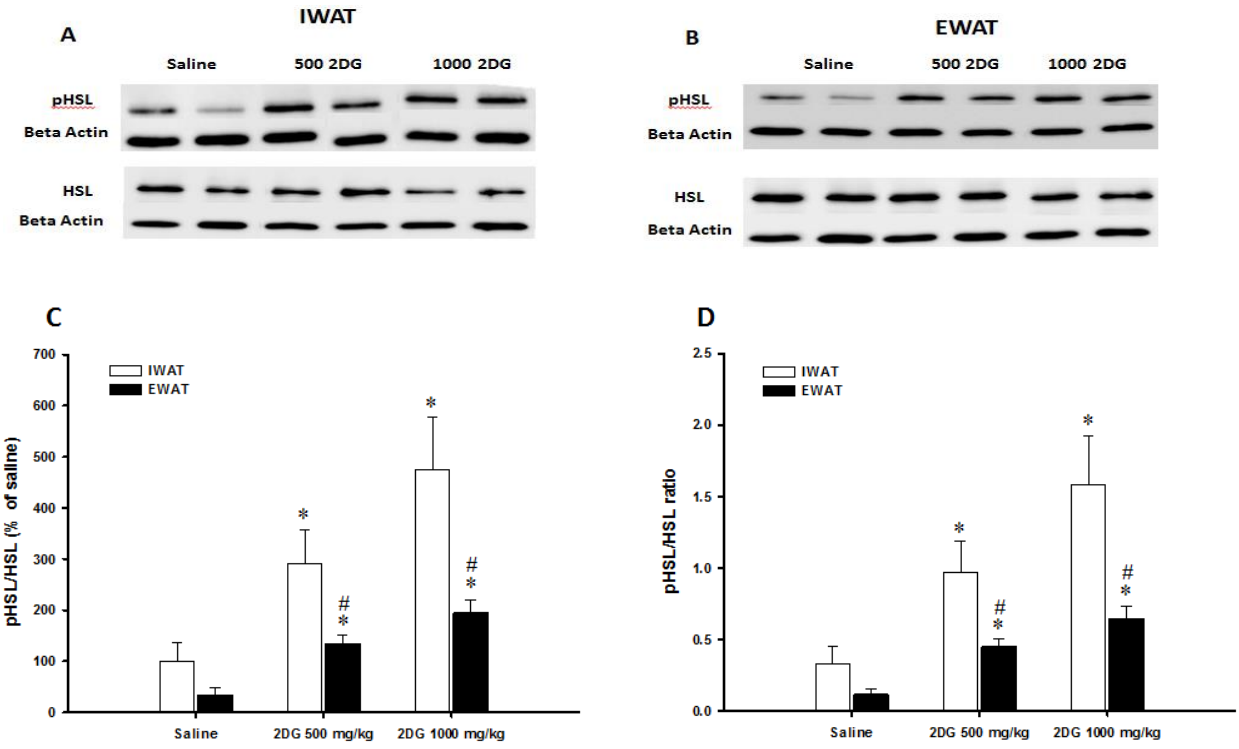

Figure 8: *Western blot analysis of WAT.*
Western blot analysis of HSL and pHSL in IWAT and EWAT with 2DG treatment A. Immunoblot of pHSL, HSL, and beta-actin protein bands in IWAT. B Immunoblot of pHSL, HSL, and beta-

*actin protein bands in EWAT. C: Western blot with ratio of HSL/pHSL taken as percent of saline. D: Western blot with ratio of HSL/pHSL taken as ratio *P<0.05 vs Saline, #P<0.05 vs 500mg/kg.*

4 DISCUSSION

Collectively, using two distinct monosynaptic retrograde tract tracers, FG and FB, we for the first time revealed separate and shared innervation of both IWAT and EWAT of Siberian hamsters by the SNS and SS ganglia. Our results suggest that IWAT is more innervated than EWAT by both the SS and SNS. We also showed that 2DG dose-dependently increased the SNS drive to the WAT up to two hours with faded activation in the SS ganglia, implying the initial SS role in sensing the SNS drive. The higher innervation of the IWAT resulted in higher SNS drive and, thus, lipolytic rate within the IWAT compared with the EWAT, which support the notion of faster fat mobilization in the subcutaneous over inner fat depots.

In agreement with the innervation study of IWAT and EWAT (38), we showed similar separate patterns of innervation by the SNS ganglia. Our tracing studies indicated more innervation of IWAT at T13 and L1 ganglia in concordance with the above-mentioned study; however, we did not confirm higher EWAT innervation emanating from L2 or L3 ganglia. Our results showed that both the total number and percentage of innervation SNS innervation to IWAT was greater for each ganglia analyzed. The dissimilarities between the two studies could arise from the difference in the amount of tracer injected in which IWAT was treated (5 μl previously vs 8 μl in the current study). The SS innervation of the IWAT and EWAT were similar to that of the SNS innervation of the IWAT being most innervated in all the ganglia in comparison to the EWAT. Our results demonstrated, that the IWAT appeared to be ~2-fold more innervated as compared with the EWAT by both the SS and SNS. Interestingly, we found that

both the SNS and SS ganglia contained roughly equal number of doubly labeled neurons (~12-17%) showing neuroanatomical evidence of crosstalk between two fat depots.

We previously showed that 2DG rapidly activates sensory afferents within 5-10 minutes (36) indicating that sensory afferents could sense some aspects of lipolysis. In this study, we observed increased SNS activation up to two hours after 2DG administration but not in the SS. Activation in the SNS peaks at two hours post systemic 2DG (21); however, this may not be optimal for the SS if they are primarily activated. At two hours, the activation of the SS affertents of WAT may have exhibited diminished effects. The SNS drive to the WAT is not uniform and, previously, we found that 2DG differently affects lipolysis in different fat depots (10).That is, NETO/lipolysis increases responding to 2DG treatment occur specifically in the IWAT but not in the EWAT when we used 2DG at 500 mg/kg (10). Nevertheless, in the current study we demonstrated that the higher 2DG dose (1000 mg/kg) is capable to trigger lipolysis.

Therefore, we conclude that the EWAT may possess a higher threshold to 2DG in order to initiate lipolysis. In addition to establishing SNS activation we measured the lipolytic properties within both IWAT and EWAT by examining the ratio of pHSL and HSL, *in vivo* markers of lipolysis, for each fat pad after 2DG. We showed a significant dose-dependent increase of lipolysis in both the IWAT and EWAT in response to 2DG stimulus. Increases in the SNS activation to both IWAT and EWAT were exhibited specifically in T13 and L1 ganglia. The lipolytic rate in the IWAT was approximately two times greater than in the EWAT for both 2DG treatment groups. It appears that more adipocytes from IWAT-SNS and SS innervation contributed to higher lipolytic response, thus supporting the notion of trivial dichotomic distinctions between the faster mobilized subcutaneous WAT and slower mobilized visceral WAT.

Collectively, our results show persuasive evidence of the IWAT and EWAT SNS-SS neural crosstalk with a coordinated control of lipolytic function. Additionally, we demonstrated that the IWAT appeared to be profoundly more innervated by either the SNS or the SS, thus, indicating higher lipolityc capacities of the subcutaneous WAT in response to 2DG. Finally, our tracing studies combined with the c-Fos immunostaining revealed specific ganglia contributing to the innervation of both fat depots, therefore, providing a model system with which to determine the lipolytic properties of distinct fat pad in response to various metabolic stimuli, such as glucoprivation, cold exposure and starvation. It is our hope that further understanding of the SNS-SS interaction in relation with WAT innervations could shed light on the intrinsic nature of WAT to maximize fat mobilization to reverse obesity and associated metabolic diseases.

REFERENCES

1. **Arner P**. Human fat cell lipolysis: biochemistry, regulation and clinical role. *BestPractResClinEndocrinolMetab* 19: 471-482, 2005.
2. **Bamshad M, Aoki VT, Adkison MG, Warren WS, and Bartness TJ**. Central nervous system origins of the sympathetic nervous system outflow to white adipose tissue. *AmJPhysiol* 275: R291-R299, 1998.
3. **Bartness TJ**. Photoperiod, sex, gonadal steroids and housing density affect body fat in hamsters. *Physiology and Behavior* 60: 517-529, 1996.
4. **Bartness TJ, Demas GE, and Song CK**. Central nervous system innervation of white adipose tissue. In: *Adipose Tissue*, edited by Klaus S. Georgetown, TX: Landes Bioscience, 2001, p. 116-130.
5. **Bartness TJ, Demas GE, and Song CK**. Seasonal changes in adiposity: the roles of the photoperiod, melatonin and other hormones and the sympathetic nervous system. *ExpBiolMed* 227: 363-376, 2002.
6. **Bartness TJ, Hamilton JM, Wade GN, and Goldman BD**. Regional differences in fat pad responses to short days in Siberian hamsters. *AmJPhysiol* 257: R1533-R1540, 1989.
7. **Bartness TJ, Morley JE, and Levine AS**. Effects of food deprivation and metabolic fuel utilization on the photoperiodic control of food intake in Siberian hamsters. *Physiology and Behavior* 57: 61-68, 1995.
8. **Bartness TJ, and Wade GN**. Photoperiodic control of seasonal body weight cycles in hamsters. *NeurosciBiobehavRev* 9: 599-612, 1985.
9. **Bowers RR, Festuccia WTL, Song CK, Shi H, Migliorini RH, and Bartness TJ**. Sympathetic innervation of white adipose tissue and its regulation of fat cell number. *AmJPhysiol* 286: R1167-R1175, 2004.
10. **Brito NA, Brito MN, and Bartness TJ**. Differential sympathetic drive to adipose tissues after food deprivation, cold exposure or glucoprivation. *AmJPhysiol RegulIntegrComp Physiol* 294: R1445-R1452, 2008.
11. **Carmen GY, and Victor SM**. Signalling mechanisms regulating lipolysis. *Cell Signal* 18: 401-408, 2006.
12. **Collins S, Migliorini RH, and Bartness TJ**. Mechanisms controlling adipose tissue metabolism by the sympathetic nervous system: anatomical and molecular aspects. In: *Handbook of Contemporary Neuropharmacology*, edited by Sibley D, Hanin I, Kuhar M, and Skolnick P. New York: John Wiley, 2007, p. 785-814.
13. **Correll JW**. Adipose tissue: ability to respond to nerve stimulation in vitro. *Science* 140: 387-388, 1963.
14. **Demas GE, and Bartness TJ**. Novel method for localized, functional sympathetic nervous system denervation of peripheral tissue using guanethidine. *JNeurosciMethods* 112: 21-28, 2001.
15. **Finkelstein EA, Trogdon JG, Cohen JW, and Dietz W**. Annual medical spending attributable to obesity: payer-and service-specific estimates. *Health Aff(Millwood)* 28: 822-831, 2009.
16. **Fishman RB, and Dark J**. Sensory innervation of white adipose tissue. *AmJPhysiol* 253: R942-R944, 1987.

17. **Goldstein LB, Bushnell CD, Adams RJ, Appel LJ, Braun LT, Chaturvedi S, Creager MA, Culebras A, Eckel RH, Hart RG, Hinchey JA, Howard VJ, Jauch EC, Levine SR, Meschia JF, Moore WS, Nixon JV, and Pearson TA**. Guidelines for the primary prevention of stroke: a guideline for healthcare professionals from the American Heart Association/American Stroke Association. *Stroke* 42: 517-584, 2011.
18. **Lafontan M, and Berlan M**. Fat cell adrenergic receptors and the control of white and brown fat cell function. *Journal of Lipid Research* 34: 1057-1091, 1993.
19. **Langin D**. Adipose tissue lipolysis as a metabolic pathway to define pharmacological strategies against obesity and the metabolic syndrome. *PharmacolRes* 53: 482-491, 2006.
20. **Mauer MM, Harris RBS, and Bartness TJ**. The regulation of total body fat: lessons learned from lipectomy studies. *NeurosciBiobehavRev* 25: 15-28, 2001.
21. **Mei Q, Mundinger TO, Kung D, Baskin DG, and Taborsky GJ, Jr.** Fos expression in rat celiac ganglion: an index of the activation of postganglionic sympathetic nerves. *AmJ Physiol EndocrinolMetab* 281: E655-E664, 2001.
22. **Morgan PJ, Ross AW, Mercer JG, and Barrett P**. Photoperiodic programming of body weight through the neuroendocrine hypothalamus. *J Endocrinol* 177: 27-34, 2003.
23. **Murphy KT, Schwartz GJ, Nguyen NL, Mendez JM, Ryu V, and Bartness TJ**. Leptin-sensitive sensory nerves innervate white fat. *AmJPhysiol EndocrinolMetab* 304: E1338-E1347, 2013.
24. **Ng Mea**. Global, regional, and national prevalence of overweight and obesity in children and adults during 1980–2013: a systematic analysis for the Global Burden of Disease Study 2013. *The Lancet* 384: 766-781, 2014.
25. **Nguyen NL, Randall J, Banfield BW, and Bartness TJ**. Central sympathetic innervations to visceral and subcutaneous white adipose tissue. *AmJPhysiol RegulIntegrComp Physiol* 2014.
26. **Ogden CL CM, Kit BK, Flegal KM**. Prevalence of obesity among adults: United States, 2011-2012. *NCHS Data Brief* 131: 2013.
27. **Rao GH, Thethi I, and Fareed J**. Vascular disease: obesity and excess weight as modulators of risk. *ExpertRevCardiovascTher* 9: 525-534, 2011.
28. **Reaven GM**. Insulin resistance: the link between obesity and cardiovascular disease. *MedClinNorth Am* 95: 875-892, 2011.
29. **Ryu V, and Bartness TJ**. Short and long sympathetic-sensory feedback loops in white fat. *AmJPhysiol RegulIntegrComp Physiol* 2014.
30. **Shen WJ, Patel S, Miyoshi H, Greenberg AS, and Kraemer FB**. Functional interaction of hormone-sensitive lipase and perilipin in lipolysis. *JLipid Res* 50: 2306-2313, 2009.
31. **Shi H, and Bartness TJ**. Neurochemical phenotype of sympathetic nervous system outflow from brain to white fat. *Brain ResBull* 54: 375-385, 2001.
32. **Shi H, and Bartness TJ**. White adipose tissue sensory nerve denervation mimics lipectomy-induced compensatory increases in adiposity. *AmJPhysiol* 289: R514-R520, 2005.
33. **Shi H, Song CK, Giordano A, Cinti S, and Bartness TJ**. Sensory or sympathetic white adipose tissue denervation differentially affects depot growth and cellularity. *AmJPhysiol* 288: R1028-R1037, 2005.
34. **Song CK, and Bartness TJ**. CNS sympathetic outflow neurons to white fat that express melatonin receptors may mediate seasonal adiposity. *AmJPhysiol* 281: R666-R672, 2001.

35. **Song CK, Jackson RM, Harris RB, Richard D, and Bartness TJ**. Melanocortin-4 receptor mRNA is expressed in sympathetic nervous system outflow neurons to white adipose tissue. *AmJPhysiol RegulIntegrComp Physiol* 289: R1467-R1476, 2005.
36. **Song CK, Schwartz GJ, and Bartness TJ**. Anterograde transneuronal viral tract tracing reveals central sensory circuits from white adipose tissue. *AmJPhysiol RegulIntegrComp Physiol* 296: R501-R511, 2009.
37. **Weiner J**. Limits to energy budget and tactics in energy investments during reproduction in the Djungarian hamster (Phodopus sungorus sungorus Pallas 1770). *Symposia Zoologogical Society London* 57: 167-187, 1987.
38. **Youngstrom TG, and Bartness TJ**. Catecholaminergic innervation of white adipose tissue in the Siberian hamster. *AmJPhysiol* 268: R744-R751, 1995.
39. **Youngstrom TG, and Bartness TJ**. White adipose tissue sympathetic nervous system denervation increases fat pad mass and fat cell number. *AmJPhysiol* 275: R1488-R1493, 1998.
40. **Zalesin KC, Franklin BA, Miller WM, Peterson ED, and McCullough PA**. Impact of obesity on cardiovascular disease. *MedClinNorth Am* 95: 919-937, 2011.